# Dynamics of a Single Vortex Line in a Bose-Einstein Condensate

P. Rosenbusch, V. Bretin, and J. Dalibard
*Laboratoire Kastler Brossel,* * 24 rue Lhomond, 75005 Paris, France*
(Received 26 June 2002; published 28 October 2002)

We study experimentally the line of a single quantized vortex in a rotating prolate Bose-Einstein condensate confined by a harmonic potential. In agreement with predictions, we find that the vortex line is in most cases curved at the ends. We monitor the vortex line leaving the condensate. Its length is measured as a function of time and temperature. For a low temperature, the survival time can be as large as 10 sec. The length of the line and its deviation from the center of the trap are related to the angular momentum per particle along the condensate axis.

DOI: 10.1103/PhysRevLett.89.200403 PACS numbers: 03.75.Fi, 32.80.Pj, 67.40.Vs

The macroscopic motions of quantum and classical fluids are dramatically different. The description of a quantum fluid by a macroscopic wave function $\psi = \sqrt{\rho}e^{i\theta}$ imposes strong constraints upon its velocity field. At a position of nonvanishing density $\rho$, the velocity is related to the phase $\theta$ by $\boldsymbol{v} = \hbar\boldsymbol{\nabla}\theta/m$, where $m$ is the mass of a particle of the fluid. Hence, $\boldsymbol{\nabla} \times \boldsymbol{v} = 0$. A rotational motion of the fluid can be obtained only through the nucleation of vortex lines, along which the density is zero and around which the circulation of the velocity is quantized in units of $h/m$ [1,2].

Quantized vortices play an essential role in the dynamics of all quantum macroscopic objects. Examples are flux lines in superconductors [3], and vortex lines in superfluid liquid helium [4] and gaseous Bose-Einstein condensates (BEC) [5–9]. Among the remaining problems is the shape of a vortex/flux line and the study of its time evolution. The observation of inclined flux lines in superconductors was possible only due to recent advances in electron microscopy [10]. In gaseous BEC, one has comparably easy access to the vortex line because the density of the atom cloud is low. A few disordered vortex lines have been observed by taking tomographic images perpendicular to the long axis of a cigar shaped condensate [7]. An array of many vortex lines in a pancake shaped condensate has been observed by transverse imaging of the whole atom cloud [11].

In this Letter, we report the full length observation of a single vortex line in a cigar shaped condensate. We find that as a result of spontaneous symmetry breaking the line is generally bent. Our experimental results confirm recent predictions, in which the shape of the vortex line minimizing the energy of the gas was derived for a given rotation frequency [12–16]. We also study the time evolution of the shape of the line. As the angular momentum of the gas slowly decays, the bending of the vortex line and its deviation from the center of the trap increase. From our results, one can hope to draw some indications for the shape and dynamics of the vortex/flux line in systems where a direct observation is not yet possible.

Our $^{87}$Rb condensate is formed by radio-frequency (rf) evaporation of $10^9$ atoms in an Ioffe-Pritchard magnetic trap. The atoms are spin polarized in the $F = m_F = 2$ state. The magnetic trap has a longitudinal frequency $\omega_z/2\pi = 11.8$ Hz and a transverse frequency $(\omega_x + \omega_y)/4\pi = \omega_\perp/2\pi = 97.3$ Hz (the $x$ axis is vertical). Because gravity slightly displaces the center of the trap with respect to the magnetic field minimum, the potential in the $xy$ plane is not perfectly isotropic and we measure a 1% relative difference between $\omega_x$ and $\omega_y$.

The condensation threshold is reached at $T_c \sim 300$ nK, with $N_c \sim 2 \times 10^6$ atoms. We cool to typically $T \sim 90$ nK which corresponds to a condensate with $N_0 \sim 5 \times 10^5$ atoms and a chemical potential $\mu \sim 70$ nK. It is obtained using $\nu_f = \nu_0 + 10$ kHz as the final rf, where $\nu_0$ is the frequency at which the trap is emptied. During the rest of the experimental cycle, we maintain the evaporation rf at an adjustable level, typically $\nu = \nu_0 + 12$ kHz, to control the temperature.

Once the condensate is formed, we use an off-resonant laser beam to impose on the trapping potential an elliptic anisotropy in the $xy$ plane [6]. The wavelength of the beam is 852 nm, its power 0.1 mW, and its waist 20 $\mu$m. Acousto-optic modulators deflect the position of the beam in the $xy$ plane, thereby rotating the potential anisotropy at a frequency of $\Omega/2\pi = 70$ Hz. We apply this "laser stirrer" for 300 ms, during which ~7 vortices are nucleated [17]. The condensate then evolves freely in the magnetic trap for an adjustable time $\tau$.

The preparation of a single vortex line takes advantage of the slight static anisotropy of our magnetic trap, so that the angular momentum is not exactly a constant of motion. In a time $\tau \sim 1$–2 s, we observe a transition from a multivortex condensate to a condensate with a single vortex. This relatively long time levels the fluctuations that may occur during the nucleation process. Thereby, we are able to reproduce a condensate with a single vortex on every experimental cycle. This vortex line can then be studied for a time $\tau \leq 10$ s.

The atom distribution at $\tau$ is probed (destructively) by switching off the magnetic trap, letting the cloud expand during $t_{TOF} = 25$ ms and performing absorption imaging. Two imaging beams aligned along the $y$ and $z$ directions probe the atom cloud simultaneously [Fig. 1(a)]. The

  

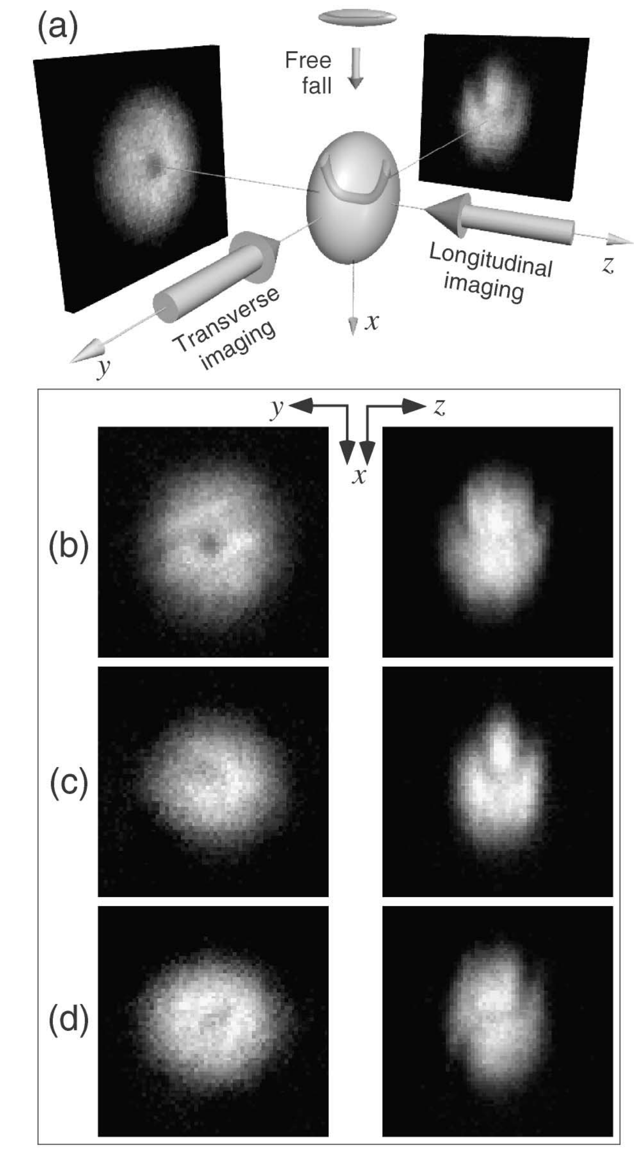


FIG. 1. (a) Schematic of the imaging system. The cigar shaped condensate is imaged after 25 ms of time of flight leading to the inversion of the ellipticity in the $xz$ plane. Two beams image the atom cloud simultaneously along the longitudinal ($z$) and transverse ($y$) directions of the initial cigar. (b)–(d) Simultaneous longitudinal and transverse images of condensates after $\tau = 4$ s (b), $\tau = 7.5$ s (c), and $\tau = 5$ s (d).

beams are combined onto a camera with the same magnification. During the expansion, the transverse dimensions $x$ and $y$ of the condensate are magnified by $\omega_\perp t_{\mathrm{TOF}} \sim 15$, while the longitudinal dimension is nearly unchanged [18]. It has been shown theoretically that the presence of a single vortex line does not alter this expansion and that the coordinates of the line are scaled by the same factors [15].

Figures 1(b)–1(d) show three condensates imaged after various times. The left column shows the "longitudinal" view along $z$, representing the atom distribution in the $xy$ plane. The right column depicts the "transverse" view taken along the $y$ direction, representing the atom distribution in the $xz$ plane. The vertical ($x$) direction is identical for all images. The transverse images show the typical atom distribution where the ellipticity is inverted with respect to the *in situ* cigar form, caused by the transverse expansion during $t_{\mathrm{TOF}}$.

As in Ref. [6], we use the longitudinal images in Fig. 1 to verify the presence of a single vortex. The transverse image in Fig. 1(b) obtained for $\tau = 4$ s shows the vortex line as a line of lower atom density. Clearly this vortex line is not straight. It rather has the shape of a wide "U." The $x$ position of the axial part of the vortex line (bottom of the U) is close to the center of the condensate. It coincides with the $x$ position of the dip in density seen in the longitudinal image. In the laboratory frame, the curved vortex line is expected to rotate around the $z$ axis with a frequency related to the angular momentum of the condensate. This is confirmed by the fact that we observe up- and downwards bending with equal probability.

Figure 1(c) shows images taken after $\tau = 7.5$ s, for which the angular momentum has decreased significantly compared to Fig. 1(b). In the longitudinal view, one sees a vortex off center and in the transverse view a narrow U, where the bottom of the U no longer extends to the center of the condensate.

Figure 1(d) shows a vortex line in the shape of an unfolded "N," observed after $\tau = 5$ s. The width of the N, which is the projection of the vortex line onto the $z$ axis, is comparable to the width of the U in Fig. 1(b). The fact that U as well as N shaped vortex lines are observed leads to the question whether the bending occurs in one plane or whether three dimensional deformations of the vortex line can also occur. We have indications that this may be the case: some transverse views (not shown here) reveal asymmetric U or N shaped vortex lines.

In order to give a quantitative analysis, we measure the distance along the $z$ direction between the two points where the vortex line leaves the condensate [Fig. 2(a)]. We do not distinguish U and N shaped vortices. Normalization by the length of the condensate along $z$ leads to the quantity $d_z$. In Fig. 2(b), we plot $d_z$ as a function of

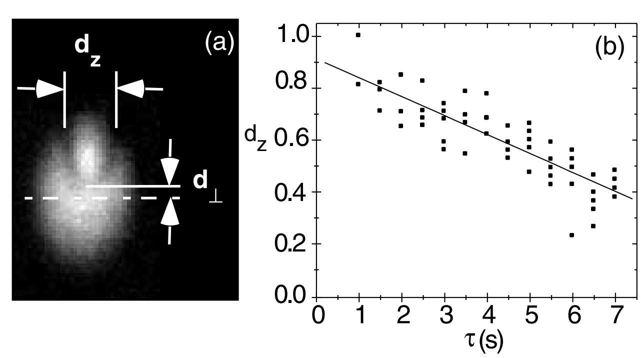


FIG. 2. (a) Schematic of the extraction of $d_z$ and $d_\perp$ from the vortex line. (b) Evolution of $d_z$ with $\tau$. Each point corresponds to a single image.

$\tau$. Each point in the plot corresponds to a single image. The small spread of the points demonstrates the reproducibility of the vortex shape. The normalized length of the vortex line, $d_z$, decreases quasilinearly with time. The number of atoms is divided by a factor 2.5 in 7 s.

Figure 2(b) shows that after $\tau = 7$ s the vortex is still present. This differs from our earlier reports [6] simply because we have used two different methods of identifying the vortex. In Ref. [6] only the longitudinal view was available. Now we find that a vortex can still be identified in the transverse view, while in the longitudinal image the density variation due to its bending is within the background fluctuations. This long lifetime is reminiscent of the MIT result [7], where a vortex array with more than 100 vortices was produced at $\tau = 0$. The number of vortices was divided by 4 in $\sim$5 s; however, a single vortex could still be detected after $\tau = 40$ s. In both experiments, it is clear that the decay time of the last vortex is much longer than that of the initial array.

We have repeated this experiment for different evaporation radio frequencies $\nu$ (implying different temperatures $T$) during the free evolution time $\tau$. At the lowest $T$ (75 nK), we observe almost exclusively U shaped vortices, while N shaped vortices occur with a significant probability for $T \geq 90$ nK. We observe a quasilinear decrease of $d_z$ for all temperatures, with a slope $\dot{d}_z$ which passes from $0.04(1)\ \mathrm{s}^{-1}$ to $0.15(3)\ \mathrm{s}^{-1}$, when $T$ varies from 75 nK ($T/T_c \sim 0.4$) to 150 nK ($T/T_c \sim 0.8$) [19]. This result can be compared to that in Ref. [20], where the decay rate of an array of $\sim 100$ vortices as a function of $T$ was measured. In Ref. [20], a 60% increase in $T$ leads to an increase by a factor 17 in the decay rate (rate $\propto T^6$). This variation is more dramatic than ours, indicating different decay mechanisms for a single vortex and for a large vortex array. In the latter case, the friction between the vortices and the thermal cloud makes the two components of the system stick together [21]. For a single vortex, the most probable scenario is that the rotation of the thermal component rapidly stops due to the residual static trap anisotropy [22]. The friction between the two components then drives the vortex line to the edge of the condensate [23].

In a last experiment, we have studied the relation between the shape of the vortex line and the average angular momentum per particle $L_z$. A given measurement consists in three experimental runs, which all start by stirring the condensate as described before and waiting for a given time $\tau$. For the first two runs of the measurement, we excite a superposition of the two quadrupole surface modes $m = \pm 2$ by a 1.9 ms flash of our laser stirrer, and we probe the quadrupole oscillation at $t_{\mathrm{osc}} = 2$ ms (first run) and $t_{\mathrm{osc}} = 9$ ms (second run) after the flash. From the precession of the condensate axes, we infer the frequency difference between the quadrupole modes, hence $L_z$ [24,25]. For the third run, we repeat the experiment without the laser flash and analyze the shape of the vortex line. As above, we extract the normalized length $d_z$ of the vortex line along the $z$ axis. We also measure the displacement $d_\perp$ of the axial part of the vortex line (bottom of the U) from the center of the condensate, and normalize it by the radius of the condensate in the $xy$ plane [Fig. 2(a)]. Since we have access only to the projection of the decentering on the $xz$ plane, we actually measure $d_\perp|\cos\alpha|$, where $\alpha$ is the azimuthal angle of the axial part of the line. We account for this geometrical factor by dividing the measured displacement by $\langle|\cos\alpha|\rangle = 2/\pi$.

Figure 3 shows $d_z$ and $d_\perp$ as functions of $L_z/\hbar$. For clarity, we group all points into bins of $L_z = 0.1\hbar$ and average over $d_z$ and $d_\perp$. The error bars give the statistical variation. The data corresponding to $L_z \leq 0.2\hbar$ are not reproducible enough and are omitted. The graph shows that $d_z$ and $L_z/\hbar$ are approximately equal. A straight ($d_z \sim 1$) and well centered ($d_\perp \ll 1$) vortex line corresponds to an angular momentum of the order of $\hbar$. When the angular momentum decreases, we measure a decentering $d_\perp \leq 0.15$ as long as $L_z > 0.5\hbar$. Below $L_z = 0.5\hbar$, $d_\perp$ rises to 0.3.

We now compare our experimental results with recent predictions for the shape of a vortex line in an inhomogeneous cigar shaped condensate [12–16]. These theoretical studies consist in looking for the ground state of the condensate in a frame rotating at an angular frequency $\Omega$. The general conclusion is that above a critical frequency $\Omega_c$ the ground state of the system has one or several vortices. The central vortex is generally bent if the trap aspect ratio $\omega_\perp/\omega_z$ is large compared to 1, which is the case in our experiment. A simple physical picture of the bending is given in Ref. [15]. A cigar shaped condensate can be viewed as a series of 2D sheets of condensate at various $z$. For each sheet, one has a 2D vortex problem leading to a critical frequency $\Omega_c^{(2D)}(z)$ above which a centered vortex is the stable solution. For a given rotation frequency $\Omega$, it can happen that a centered vortex is the minimum energy configuration for the sheets close to $z = 0$ [i.e., $\Omega_c^{(2D)}(0) < \Omega$], while it is not the case for

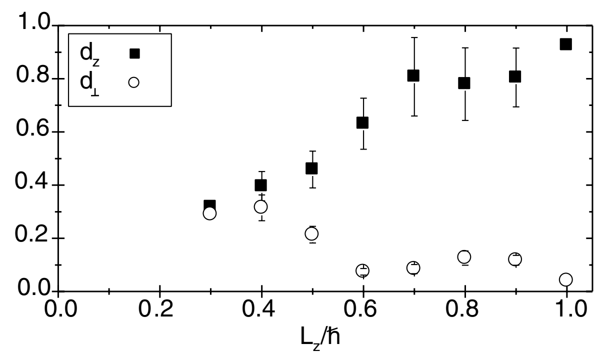


FIG. 3. Variation of $d_z$ and $d_\perp$ as functions of the average angular momentum per particle $L_z$. All measurements were binned into intervals of $L_z = 0.1\hbar$ and averaged. The error bars give the statistical spread.

the sheets close to the edges of the condensate where the atom density is lower. In this case, the vortex line minimizing the total energy is well centered for $|z| < z_c$ and is strongly bent for $|z| > z_c$, where $\Omega_c^{(2D)}(z_c) = \Omega$. A precursor of this bending effect has also been found in Refs. [26,27] in which a stability analysis of a straight vortex in an elongated condensate showed that some bending modes have negative energy and are thus unstable. As mentioned in Ref. [13], this bending is a symmetry breaking effect which does not depend on the presence of a rotating anisotropy and which happens even in a completely symmetric setup [28].

Our experimental procedure is somewhat different from the one considered in these theoretical studies. In our case, no rotating anisotropy is imposed onto the condensate during the relevant evolution. The stirring laser has been switched on for a short time only, at the beginning of the procedure, in order to set a nonzero angular momentum in the system. We observe the evolution of the condensate in our static trap, as the angular momentum of the gas slowly decays. Therefore, the description of our rotating condensate at time $\tau$ should correspond to a system with given $L_z$ rather than a system rotating with given $\Omega$. The states of minimal energy may differ between these two descriptions [15,29]. However, the shape of the vortex line that we observe at short time in Fig. 1(b) is remarkably similar to those predicted and plotted in Refs. [12–15]. A decentered single vortex similar to the one shown in Fig. 1(c) was also found in Ref. [14] for a given rotation range. By contrast, we did not find in the literature predictions for N shaped vortices, such as the one shown in Fig. 1(d). This probably means that an N shaped vortex is slightly more energetic than a U shaped vortex with the same angular momentum, and that it could not emerge from a procedure aiming to find the ground state of the system.

Our results also provide information on the dynamics of the vortex line and the way it escapes from the condensate. In the model of Ref. [23], the decay is due to the coupling with the nonrotating thermal component. The authors consider a spatially homogenous condensate in a cylindrical vessel. The vortex line, assumed to be straight, spirals out of the condensate. The bending of the line that we observe experimentally may change qualitatively the picture, since we find that the decay occurs first by an increased bending and, only in a second step, by a deviation of the center of the line (bottom of the U) from the center of the condensate.

In conclusion, we have reported the observation of the full line of a single quantized vortex. We have related its shape (bending and deviation from center) to the angular momentum of the system. Our results should help modeling the dissipative evolution of a rotating Bose-Einstein condensate.

We thank Y. Castin, F. Chevy, and G. Shlyapnikov for useful discussions. P. R. acknowledges support by the EC (Contract No. HPMF CT 2000 00830) and Alexander-von-Humbolt Stiftung. This work is partially supported by CNRS, Collège de France, Région Ile de France, DGA, DRED, and EU (TMR network ERB FMRX-CT96-0002).

*Unité de Recherche de l'Ecole normale supérieure et de l'Université Pierre et Marie Curie, associée au CNRS.

[1] L. Onsager, Nuovo Cimento Suppl. **6**, 249 (1949).
[2] R. P. Feynman, in *Progress in Low Temperature Physics*, edited by C. J. Gorter (North-Holland, Amsterdam, 1955), Vol. 1, Chap. 2.
[3] M. Tinkham, *Introduction to Superconductivity* (McGraw-Hill, New York, 1996).
[4] R. J. Donnelly, *Quantized Vortices in Helium II* (Cambridge University, Cambridge, 1991).
[5] M. R. Matthews *et al.*, Phys. Rev. Lett. **83**, 2498 (1999).
[6] K.W. Madison *et al.*, Phys. Rev. Lett. **84**, 806 (2000).
[7] J. R. Abo-Shaeer *et al.*, Science **292**, 476 (2001); C. Raman *et al.*, Phys. Rev. Lett. **87**, 210402 (2001).
[8] E. Hodby *et al.*, Phys. Rev. Lett. **86**, 2196 (2001).
[9] P. C. Haljan *et al.*, Phys. Rev. Lett. **87**, 210403 (2001).
[10] A. Tonomura *et al.*, Nature (London) **412**, 620 (2001); A. Tonomura *et al.*, Phys. Rev. Lett. **88**, 237001 (2002).
[11] P. Engels *et al.*, cond-mat/0204449.
[12] J. J. García-Ripoll and V. M. Pérez-García, Phys. Rev. A **63**, 041603 (2001).
[13] J. J. García-Ripoll and V. M. Pérez-García, Phys. Rev. A **64**, 053611 (2001).
[14] A. Aftalion and T. Riviere, Phys. Rev. A **64**, 043611 (2001).
[15] M. Modugno *et al.*, cond-mat/02033597.
[16] A. Aftalion and R. L. Jerrard, cond-mat/0204475.
[17] K.W. Madison *et al.*, Phys. Rev. Lett. **86**, 4443 (2001).
[18] Y. Castin and R. Dum, Phys. Rev. Lett. **77**, 5315 (1996).
[19] The precision of our measurement was not high enough to discriminate between a quadratic variation ($\dot{d}_z \propto T^2$) and a linear variation with an offset ($\dot{d}_z \propto T - T_0$).
[20] J. R. Abo-Shaeer *et al.*, Phys. Rev. Lett. **88**, 070409 (2002).
[21] O. N. Zhuravlev *et al.*, Phys. Rev. A **64**, 053601 (2001).
[22] D. Guéry-Odelin, Phys. Rev. A **62**, 033607 (2000).
[23] P. O. Fedichev and G.V. Shlyapnikov, Phys. Rev. A **60**, R1779 (1999).
[24] F. Chevy *et al.*, Phys. Rev. Lett. **85**, 2223 (2000).
[25] F. Zambelli and S. Strigari, Phys. Rev. Lett. **81**, 1754 (1998).
[26] A. A. Svidzinsky and A. L. Fetter, Phys. Rev. A **62**, 063617 (2000).
[27] D. L. Feder *et al.*, Phys. Rev. Lett. **86**, 564 (2001).
[28] The small static trap anisotropy should not influence the symmetry breaking occuring in the rotating frame.
[29] D. A. Butts and D. S. Rokshar, Nature (London) **397**, 327 (1999).